

ARTICLE TYPE

Mathematical based control method and performance analysis of a novel hydromechatronics driving system Micro-Independent Metering

Karem Abuowda² | Mihai Dupac*¹ | Siamak Noroozi¹ | Philip Godfrey²¹Department of Design and Engineering,
Bournemouth University, Dorset, UK²Design Engineering Department,
HYDRECO Hydraulic Ltd, Dorset, UK**Correspondence***Mihai Dupac, Talbot Campus, Fern
Barrow, Poole BH12 5BB. Email:
mdupac@bournemouth.ac.uk**Present Address**Talbot Campus, Fern Barrow, Poole BH12
5BB, UK**Abstract**

This paper aims to investigate the performance of a hydraulic actuator controlled by the novel system micro-independent metering (MIM). This analysis has been performed by comparing the models of two systems which are the traditional independent metering, that depends on poppet valve, and the new hydro-mechatronics system micro-independent metering, that relies on a stepped rotary flow control valve. In general, independent metering is a hydraulic control system which guarantees a separation between the meter-in and the meter-out of the hydraulic actuator. A Valvistor valve, a special type of Poppet valves, was developed to be embedded into the independent metering (IM) system. This valve has controllability and stability shortcomings which prevent the system from spreading in the industrial applications. The Valvistor valve performance is highly affected by the fluid disturbances because the fluid is considered as a part of its control elements. A stepped rotary flow control valve has been developed to control hydraulic flow rate. The valve composed of a rotary orifice attached to a stepper motor. Using this valve instead of the traditional poppet type has led to a new configuration, that is termed by micro-independent metering. This form improves the hydraulic cylinder velocity performance by rejecting the fluid disturbances effect on the control circuit.

KEYWORDS:

Independent Metering, Micro-Independent Metering, Control Algorithm, Fluid Mechanics

1 | INTRODUCTION

Hydraulic systems are important elements that indirectly contribute to the quality of human life. They are heavily used for a variety of applications ranging from construction to industrial, military, aerospace, and earth moving applications due to their unique and valuable characteristics. Compared to electrical actuators, hydraulic drives are characterized by high load capabilities, high power to weight ratio and robustness^{1,2}. However, they still suffer from some shortcomings, such as energy losses and nonlinearities which make the control system more challengeable^{2,3}. To overcome the hydraulic drives drawbacks, hydraulic individualization methodology is used. It improves the power density, robustness and flexibility. Individualization can be split into displacement and valve control⁴. Information about displacement individualization can be obtained from^{4,5,6}.

1.1 | Literature Overview

Regarding individualization using hydraulic control valves, which is the point of this research, there are three main types of individualization. The first approach is common metering edge, which is the traditional control approach. Each actuator is controlled by one valve. Due to the mechanical connection between the metering edges of the actuator using traditional valves, the system has one degree of freedom which means that one chamber pressure is controlled⁷. This configuration limits the system flexibility, but increases the robustness⁸. To improve the efficiency and the energy saving, the trend was to break the mechanical connection between the meter-in and the meter-out edges, which is why it is called IM. Different terms are used for IM as separate metering, programmable valves, multifunction valves and separate meter-in separate meter-out control^{9,10,11}.

Researches on IM systems has been conducted with various approaches. The first improvement was quantities decoupling¹². Many techniques were improved for decoupling such as LQ technique and pressure feedback^{6,13}. The effects of feedback linearization and open loop control were investigated by Jouni and Tapio¹⁴ and by Haibo and Zhang¹⁵. Besides, adaptive control, which is an important field, was used for these systems^{9,16,17}. On the other hand, Tabor developed a quasi-static mathematical technique for IM¹⁸. Improving this model was by inserting continuous mode switching¹⁹. A high technology improvement for IM was by inserting digital hydraulics²⁰. Every actuator or consumer is actuated by four digital fluid control unit (DFCU) which contains an array of on/off valves²¹. There was also a new system based on a hybrid concept such as STEAM^{6,22}.

Different control parameters can be used for IM. These parameters can be separated into flow, pressure difference and displacement control. As the separation of actuator metering increased the degree of freedom, different control strategies can be applied and investigated on the system. A first approach, known as a Feed-forward control, is generally used^{4,23}. The second type, a closed loop control feedback Single Input Single Output (SISO), ensure that the output follows the trajectory command. The last one, which is the Multiple Input Multiple Output (MIMO), is a closed loop control system. It is used to control more than one target variable where different states are controlled at the same time in the IM. These states are coupled together. The decoupling between them can be performed using MIMO control.

Hydraulic valves used to implement IM can be classified into 3/3 and 2/2 valves⁸. These are used to make different forms of decoupling between the input and the output. The first iteration to implement IM using 4/3 valves was by Monsun-Tison²³, and the system called MONTI. An example of IM configuration using two 4/3 valves is Caterpillar patent²⁴. Then, application of 3/3 valves were introduced by EATON company, and 2/2 valves were developed by many companies such as Deere, Moog and Caterpillar²⁵. These valves are cartridge poppets or Valvistor are widely used for IM control. A block arrangement which contains four valves for every actuator was developed by Caterpillar^{26,27}. A programmable valve represents a configuration of a five electronically controlled poppet valve²⁸. The performance of a programmable valve²⁹ was evaluated in^{30,23}. After manufacturing, a deviation in performance affecting the IM system overall was noticed³¹. A novel auto-calibration state-trajectory control method for IM uses a four poppet valve configuration or a Wheatstone bridge³². Inserting electronics and sensors to IM valves improves the controllability and overall system performance³³. Using electronics and sensors in these hydraulic systems increases the failure due to the harsh environment, and to overcome this drawback a failure operational control algorithm was considered³⁴.

Based on this review, it is obvious that the current trend of research and development is to introduce new control method or techniques, which reduces some shortcomings using the traditional types of control valves. At the same time, there is a new trend to use rotary type valves similar with the one shown in Figure 1 (for more information see^{35 36 37}). This valve can be used to develop a programmable configuration of the IM system.

The aim of this paper is to study the effect of this system on a hydraulic actuator performance. This study relies on comparing the velocity performance of two models which are the traditional IM, using the Valvistor valve, and the new IM system, using the stepped rotary valve, MIM.

The mathematical analysis of the MIM method is presented in Section 2. Section 3 introduces the new stepped rotary flow control valve and the traditional Valvistor valve mathematical models. Section 4 considers the model based performance and the comparison between the MIM and IM, followed in Section 5 by the discussion and in Section 6 by the conclusion.

2 | MICRO-INDEPENDENT METERING MATHEMATICAL ANALYSIS

The IM is a hydraulic configuration which aims to control a velocity of hydraulic actuator and saves energy by allowing energy regeneration or recuperation. The energy regeneration is performed when outlet fluid from the actuator is recirculated and inserted into the same actuator or another in the machine. IM technique relies on five modes of operation which are Power

Extension (PE), Power Retraction (PR), High side regeneration extension (HSRE), low side regeneration retraction (LSRR), and Low side extension (LSRE). The PE and PR are the most power consumer, while other modes regenerate energy from the cylinder chamber to the another. As shown in Figure 2 , the operation modes can be split into normal where no fluid is recirculated and regeneration where fluid is recirculated. The PE is performed by supplying fluid from the pump to the actuator head chamber using inlet port, while the fluid is drained from the actuator to the tank using the outlet branch. The next operation mode is the PR which is the opposite of the PE. The HSRE is shown in Figure 2 . The regeneration is achieved when the fluid is passed from the rod chamber to the head chamber using the high connection point of the bridge. If the recirculated flow is not enough, the difference is supplied by the pump itself. The low side regeneration appears when the fluid regeneration is performed at the low connection point. The low side regeneration has two modes which are the LSRR mode and the LSRE mode. The LSRE happens when the load is moving up and the gravity is being resisted. The LSRR appears when load is moving down using its gravity. The modes are shown in Figure 2 . The mathematical representation of these modes can be divided into:

1. The modes limitations.
2. The quasi-static representation.
3. The anti-cavitation force representation.

2.1 | Performance limits of the Operation Modes

The force and velocity limits of the five modes are shown in Figure 3 , the PE and the HSRE are in the first quadrant, and their power and velocity limits³⁸ are as follows,

$$[F_{PE}, V_{PE}] = \left[P_{s,max} A_a, \frac{q_{s,max}}{A_a} \right] \quad (1)$$

$$[F_{HSRE}, V_{HSRE}] = \left[P_{s,max} (A_a - A_b), \frac{q_{s,max}}{A_a - A_b} \right] \quad (2)$$

. The second quadrant includes the LSRR. Its power and velocity limits can be describe according to,

$$[F_{LSRR}, V_{LSRR}] = \left[F_l, \frac{q_{LSRR}}{A_b} \right] \quad (3)$$

The LSRE mode has two velocity limits, the first when the return pressure is build up from another actuator return flow, or the overrunning load is high enough to generate the fluid flow. The PR mode depends on the pump flow. Both modes are presented by the following equations,

$$[F_{PR}, V_{PR}] = \left[P_{s,max} \cdot A_b, \frac{q_{s,max}}{A_b} \right] \quad (4)$$

$$[F_{LSRE}, V_{LSRE}] = \left[F_l \cdot A_b, \min \left(\frac{q_{LSRE_1}}{A_a}, \frac{q_{LSRE_2}}{A_b} \right) \right] \quad (5)$$

where F is the force, V is the velocity, Q is the fluid flow rate, A_a is the head chamber area, A_b is the rod chamber area, P_a is the head chamber pressure, P_b is the rod chamber pressure, and F_l is the applied load. Changing between these modes is based on determining the applied force value

$$F = (P_a A_a - P_b A_b) \quad (6)$$

calculated using the pressure in the actuator's chambers. The threshold between the power extension and the sigh side regeneration extension can be defined by

$$HPS = P_s (A_a - A_b) \quad (7)$$

where P_s is the pump pressure.

The mode selection procedure is represented in Algorithm 1.

2.2 | Quasi-Static Mathematical Modes Representation

In the PE mode, the active valves are K_{sa} which is the inlet and K_{bt} which is the outlet. The equivalent representation of the circuit is shown in Figure 4 . According to⁴⁰ the pressure difference and flow rate across the valves can be considered as follow,

Algorithm 1 The Mode Selection Algorithm:

```

1: procedure MODESELECTION( $P_a, P_b, A_a, A_b, Speed$ )
2:   if  $Speed < 0 \ \& \ F < 0$  then
3:      $Mode \leftarrow LSRR$ 
4:   else if  $Speed < 0 \ \& \ F > 0$  then
5:      $Mode \leftarrow PR$ 
6:   else if  $Speed > 0 \ \& \ F > 0$  then
7:      $Mode \leftarrow LSRE$ 
8:   else if  $Speed > 0 \ \& \ F < 0$  then
9:     if  $-F \geq HPRE$  then
10:       $Mode \leftarrow PE$ 
11:    else
12:       $Mode \leftarrow HSRE$ 
13:    end if
14:   else
15:      $NoAction$ 
16:   end if
17: return  $Mode$ 
18: end procedure

```

$$\begin{aligned}
\Delta P_1 &= P_s - P_a, & \Delta P_2 &= P_b - P_r \\
q_{in} &= K_{sa} \sqrt{\Delta P_1} = K_{sa} \sqrt{P_s - P_a} = A_a \dot{x} \\
q_{out} &= K_{bt} \sqrt{\Delta P_2} = K_{bt} \sqrt{P_b - P_r} = A_b \dot{x}
\end{aligned} \tag{8}$$

where K_{sa} and K_{bt} are the flow conductivity factors.

The Newton's second law indicates that the $\sum F = ma$ which can be represented as follows,

$$P_s A_a - P_r A_b = \Delta P_1 A_a + (P_a A_a - P_b A_b) + \Delta P_2 A_b \tag{9}$$

By dividing the cylinder chambers area, $R = A_a/A_b$ one can obtain

$$RP_s - P_r = R\Delta P_1 + (RP_a - P_b) + \Delta P_2 \tag{10}$$

$$(RP_s - P_r) + (-RP_a + P_b) = R\Delta P_1 + \Delta P_2 \tag{11}$$

where P_r is the tank pressure.

The equivalent pressure P_{eq} of the circuit, based on Equation(11) and Equation(8) is

$$P_{eq} = (RP_s - P_r) + (-RP_a + P_b) = R\Delta P_1 + \Delta P_2 = R \frac{q_{in}^2}{K_{sa}^2} + \frac{q_{out}^2}{K_{bt}^2} \tag{12}$$

Considering the cylinder chambers area, $R = A_a/A_b$ and Equation (8) one can calculate R as

$$R = \frac{q_{in}}{q_{out}} \tag{13}$$

From Equation (12) and Equation (13) one can obtain

$$P_{eq} = \frac{R^3 q_{out}^2}{K_{sa}^2} + \frac{q_{out}^2}{K_{bt}^2} = q_{out}^2 \left[\frac{R^3 K_{bt}^2 + K_{sa}^2}{K_{sa}^2 K_{bt}^2} \right] \tag{14}$$

Rearranging Equation (14) the parameters q_{out} , K_{eq} , and P_{eq} can be written as

$$q_{out} = \frac{K_{sa} K_{bt}}{\sqrt{(R^3 K_{bt}^2) + K_{sa}^2}} = K_{eq} \sqrt{P_{eq}} \tag{15}$$

$$K_{eq} = \frac{K_{sa}K_{bt}}{\sqrt{(R^3K_{bt}^2) + K_{sa}^2}} \quad (16)$$

$$P_{eq} = (RP_s - P_r) + (-RP_a + P_b) \quad (17)$$

Combining Equation (8) and Equation (15) the flow conductance is represented by

$$K_{eq} = \frac{A_b\dot{x}}{\sqrt{P_{eq}}} = \frac{A_b\dot{x}}{\sqrt{(RP_s - P_r) + (-RP_a + P_b)}} \quad (18)$$

Based on Equation (16) and Equation (18), the K_{eq} relies on both valves working simultaneously, and it's value represents all the possible combination of the valves conductance, flow rates, to achieve the required piston speed. It also relies on the values of the supply pressure, return pressure, and both chamber pressures. To stop the piston, at least one of the two valves should be closed completely.

In the PR mode, the two valves used to achieve the required speed are K_{sb} in the inlet port and K_{at} in the outlet port. The equivalent pressure P_{eq} and conductance k_{eq} of the circuit could be written as

$$P_{eq} = (P_s - RP_r) + (-P_b + RP_a),$$

$$K_{eq} = -\frac{A_b\dot{x}}{\sqrt{(P_s - RP_r) + (-P_b + RP_a)}}. \quad (19)$$

The HSRE mode is implemented using the two valves K_{sa} , and K_{sb} . Considering the same analysis, the equivalent pressure P_{eq} and conductance k_{eq} of the circuit are obtained as

$$P_{eq} = (R - 1)P_s + (-RP_a + P_b),$$

$$K_{eq} = \frac{A_b\dot{x}}{\sqrt{P_{eq}}} = \frac{A_b\dot{x}}{\sqrt{(R - 1)P_s + (-RP_a + P_b)}}. \quad (20)$$

The same analysis is applied to the LSRE mode, but the used valves are K_{at} and K_{bt} to achieve the required speed. The equivalent pressure P_{eq} and conductance k_{eq} of the circuit are now

$$P_{eq} = (R - 1)P_r + (-RP_a + P_b),$$

$$K_{eq} = \frac{A_b\dot{x}}{\sqrt{P_{eq}}} = \frac{A_b\dot{x}}{\sqrt{(R - 1)P_r + (-RP_a + P_b)}}. \quad (21)$$

The LSRR is implemented using the valves K_{at} and K_{bt} . In this case, the equivalent pressure P_{eq} and conductance k_{eq} of the circuit are

$$P_{eq} = -(R - 1)P_r + (+RP_a - P_b),$$

$$K_{eq} = -\frac{A_b\dot{x}}{\sqrt{P_{eq}}} = \frac{A_b\dot{x}}{\sqrt{-(R - 1)P_r + (+RP_a - P_b)}}. \quad (22)$$

2.3 | Anti-Cavitation Analysis

Cavitation is an obstacle that appears when one of the chambers expands at rate faster than the fluid filling rate. When cavitation appears, the system losses the control-ability as the mathematical representation can't be implemented. To overcome this, the pressure in the inlet chamber should be reduced to the minimum value. This depends on the ratio between the two used valves in each mode. If the cavitation occurs on a defined ratio, then changing this ratio is necessary to avoid it⁴¹.

In the PE mode, the aviation occurs when the cylinder direction movement is in the same of the load. The load force F_L that causes cavitation is

$$F_L = \left(\frac{\alpha}{R}\right)^2 A_b P_s + P_r A_b + F_f. \quad (23)$$

where α is the sensitivity factor, and F_f is the friction force.

The cavitation in PR mode appears when the $P_b \leq 0$. The applied load can be represented by the equation,

$$F_L = \left(\frac{\alpha}{R}\right)^2 A_a P_s + A_a P_r + F_f. \quad (24)$$

For the HSRE, the cavitation appears when the $P_a \leq 0$ then,

$$F_l = \left[1 + \left(\frac{\alpha}{R} \right)^2 \right] A_b P_s + F_f. \quad (25)$$

The LSRE mode subject to overrunning load is

$$F_l = \left[1 + \left(\frac{\alpha}{R} \right)^2 \right] A_a P_r + F_f. \quad (26)$$

The analysis in this section is used to develop the MIM programmable control algorithm - built and tested - using the Software-in-the-Loop in the next section.

2.4 | MIM control system

The control algorithm for the MIM system has been framed based on the mathematical analysis in the previous section. The main differences between the traditional control algorithm, such as Tabor¹⁸, and the MIM control algorithm are as follows:

- The traditional IM relies on infinite positioning of the valves, but the MIM depends on finite positioning of the valves.
- As there are different types of stepper motors and drivers can be embedded into the MIM, different step divisions can be selected. This allows the driver to select the step division based on his requirement under the smoothness technique. This results in changing the selection values in the main vector of the MIM algorithm according the CVD algorithm developed through this research as shown in Figure 6 .

The MIM control algorithm aims to control the velocity of the actuator which could be a cylinder or a motor⁴². Besides, it saves the system energy by implementing the regeneration modes, which are HSRE, LSRE, and LSRR. The flowchart diagram of the MIM algorithm is shown in Figure 5 , it starts by defining the resolution degree. As different stepper motors degrees can be adjusted based on the motor type and the used motor driver, setting up the degree of the stepper motor is important at the start to generate the valve conductance vector. A limit check is used in case that the selected step is not achievable by the motor driver.

Then, the measurement for this approach are the actuator chambers pressures, the pump pressure, the tank pressure, and the required velocity are collected to select the suitable operation mode. Selecting the operation mode is based on the applied load and the capability of the force and speed of every mode. After that, the conductance values of the two valves, pair for every mode, are calculated. These values should be matched to the conductance of the valve at every step of the stepper motor. The close value detection algorithm shown in Figure 5 is performed to determine the closest degree at which the valve can produce the required conductance. The activation of the valves produces the required flow resulted in the hydraulic actuator velocity.

As this control algorithm is not applicable if the cavitation appears, the anti-cavitation checking, which is performed before executing the valves, is important. In case the cavitation is detected, a new values of the valves steps have to be selected. The user or the driver of the machine has the ability to change the step resolution, smoothness activation, which could be using scroll wheel in the joystick. Finally, a StateFlow representation of the algorithm was developed using MathWorks, and it was connected with the hydraulic cylinder model which is explained in the next section.

3 | THE STEPPED ROTARY AND THE VALVISTOR VALVES MATHEMATICAL MODELS

3.1 | Mathematical modeling of the stepped rotary valve

The stepped rotary flow control valve consists of two main parts which are the stepper motor and the mechanical rotary orifice illustrated in Figure 7 . The coupling between these two subsystems requires the stepper motor to overcome the torques generated from the mechanical part. The steady state flow torque in Equation (27), the transient flow torque in Equation (28) and the friction torque in Equation (30) have been developed and evaluated in^{35,36}. Likewise, the equations representing the stepper motor are included in the state space representation in Equation (31). The steady state flow torque of the rotary spool can be expressed by

$$T_{st.fl} = \frac{2C_c \Delta p A_o R_{e.sp} \sin \theta}{1 - C_c^2} \quad (27)$$

where $T_{st.fl}$ is the steady state flow, C_c is the contraction coefficient, Δp is the pressure difference, A_o is the opening area, and $R_{e.sp}$ is the external spool radius. The transient flow $T_{tr.fl}$ can be expressed by

$$T_{tr.fl} = \frac{(R_{e.sp}^4 - R_{i.sp}^4) A_{sp.op} \rho}{R_{e.sp}} \frac{d\omega}{dt} \quad (28)$$

where $R_{e.sp}$ is the external spool radius, $R_{i.sp}$ is the internal spool radius, ω is the angular velocity, $A_{sp.op}$ is the spool opening area.

The friction torque is represented by

$$T_{fr} = \sigma_0 + \sigma_1 \frac{dZ}{dt} + \sigma_2 \omega \quad (29)$$

and

$$\frac{dZ}{dt} = \omega - \frac{\sigma_0 |\omega|}{T_c + (T_s - T_c) \exp\left(-\left(\frac{\omega}{\omega_s}\right)^2\right)} Z \quad (30)$$

where σ_0 is the stiffness coefficient, σ_1 is the damping coefficient, σ_2 is the viscous friction coefficient, ω is the angular velocity, T_c is the Coulumb friction, T_s is the static friction, ω_s is the stribek characteristics velocity, and Z is the deflection average of the asperities on two contacting surfaces.

The stepper motor model^{43,44} is given by

$$\begin{bmatrix} \frac{d\theta}{dt} \\ \frac{d\omega}{dt} \\ \frac{di_a}{dt} \\ \frac{di_b}{dt} \end{bmatrix} = \begin{bmatrix} \omega \\ \frac{1}{J} [-K_m i_a \sin(N_r \theta) + K_m i_b \cos(N_r \theta) - B\omega - T_L] \\ \frac{1}{L} [V_a - R i_a + K_m \sin(N_r \theta)] \\ \frac{1}{L} [V_b - R i_b - K_m \cos(N_r \theta)] \end{bmatrix} \quad (31)$$

where ω is the angular velocity, J is the inertia, K_m is the detent torque constant, N_r is the number of teeth, R is the resistance, T_L is the total load torque, B is the viscous friction constant, i_a is the coil A current, i_b is the coil B current, V_a is the coil A supplied voltage, and V_b is the coil B supplied voltage.

3.2 | Mathematical model of the poppet valve

The Valvistor valve has been deeply studied in^{45,46}. To understand the effect of using different valves on the IM, it is necessary to analyze the construction and the work principle of the Poppet valve "Valvistor" shown in Figure 8 . It contains two main parts which are the Pilot valve and the Main valve. The valve drive which is a PWM solenoid controls the flow in the pilot circuit. The produced flow Q_p make a pressure difference ($P_a - P_p$) across the main poppet valve m_m and cause it to move. The movement of the main poppet changes the orifice area and therefore Q_1 changes. Also the main poppet movement changes the area of the pressure feedback slot x_m . Based on the valve working principle, the hydraulic fluid is one of the control elements, and also it is an output at the same time. This is a shortcoming in this valve control-ability, and the fluid non-linearity or disturbance can affect the system performance. The valve model concluded from³⁰ was modelled as two sets of mass-spring damper systems and a compressible fluid volume between them, divided into the pilot pressure control, the main valve dynamic, and the orifice flow. Regarding the pilot pressure, it is controlled by the pilot dynamics, the pilot orifice, slot orifice flow, and inter-stage fluid compress-ability. The movement of the pilot valve is:

$$m_p \ddot{x}_p + b_p \dot{x}_p + k_p x_p = F_p + (P_p - P_b) a_p \quad (32)$$

where $F_p = K_e U_v$. The pilot valve movement produces a flow Q_p which is,

$$Q_p = K_p x_p \sqrt{P_p - P_b} + a_p \dot{x}_p = K_p x_p \sqrt{P_p - P_b} \quad (33)$$

The flow of the pressure feedback slot is represented by the orifice flow

$$Q_2 = K_s x_m \sqrt{P_a - P_p} \quad (34)$$

The pressure P_p changes at a rate described by the net flow into the volume:

$$\dot{P}_p = \frac{\beta}{v_p} (Q_2 + a_{m,1} - Q_p) = \frac{\beta}{v_p} (Q_2 - Q_p). \quad (35)$$

The main valve poppet dynamics is represented by

$$m_m \ddot{x}_m + b_m \dot{x}_m + K_m x_m = a_{m,s} P_a - a_{m,1} P_p + (a_{m,1}) P_b + d_F \quad (36)$$

where x_m is the main movement, P_p is the pilot pressure, P_a is the inlet pressure, and the flow force d_F . Finally, the flow through the main orifice is determined by

$$Q_1 = K_m x_m \sqrt{P_a - P_b} \quad (37)$$

The valve model parameters values are collected from⁴⁵. As indicated by Equation (32), the hydraulic fluid disturbances are part of the system dynamic and affects its performance, so this is the main point of performance comparison.

4 | MODEL BASED PERFORMANCE COMPARISON

The effect of the MIM technique, and how it improves the performance of the hydraulic actuator is presented next. The effect can be detected by applying the IM using the Valvistor valve and the MIM on the same actuator with the same conditions. The analysis starts by designing two IM models for the same cylinder with the same loading conditions, and implement one of the operation modes. The selected mode is the power extension mode, so the activated valves are the one between the pump and the head chamber inlet, and the one between the rod chamber and the tank, which is the outlet. Disturbances inserted into the two model to recognize the difference in performance are considered. These disturbances are mainly due to the fluid non-linearity caused by heat, air, or machine vibration.

4.1 | Mathematical model of the actuator

The mathematical representation of the hydraulic actuator^{19,47} can be explained as follows:

- Since the IM configuration is four valves connected to one cylinder, the four orifices flows rates are

$$\begin{aligned} Q_{sa} &= K_{sa} \sqrt{(P_s - P_a)} \operatorname{sgn}(P_s - P_a), \quad Q_{sb} = K_{sb} \sqrt{(P_s - P_b)} \operatorname{sgn}(P_s - P_b) \\ Q_{at} &= K_{at} \sqrt{(P_a - P_r)} \operatorname{sgn}(P_a - P_r), \quad Q_{bt} = K_{bt} \sqrt{(P_b - P_r)} \operatorname{sgn}(P_b - P_r). \end{aligned} \quad (38)$$

- The compressibility of the actuator can be written as

$$Q_{ca} = \frac{V_{a0} + A_a x}{B_e} \dot{P}_a, \quad Q_{cb} = \frac{V_{b0} - A_b x}{B_e} \dot{P}_a. \quad (39)$$

- The conversion of mass can be expressed by

$$Q_{sa} - Q_{at} - Q_L = Q_{ca} + A_a \dot{x}, \quad Q_{sb} - Q_{bt} + Q_L = Q_{cb} - A_b \dot{x}. \quad (40)$$

- From Equation (39) and Equation (40) one can write

$$\begin{aligned} Q_{sa} - Q_{at} &= \frac{V_{a0} + A_a x}{B_e} \dot{P}_a \\ Q_{sb} - Q_{bt} &= \frac{V_{b0} - A_b x}{B_e} \dot{P}_a \end{aligned} \quad (41)$$

- The conversion of momentum can be written by

$$P_a A_a - P_b A_b = M \ddot{x} + F_l + f_f \quad (42)$$

The parameters of the selected cylinder are included in Table 1.

TABLE 1 The main parameters of the selected hydraulic cylinder

Symbol	Parameter	Value	Unit
P_s	Supply pressure	20	MPa
B_e	Bulk Modulus	689.476	MPa
A_a	Head chamber area	12272	mm ²
A_b	Rod chamber area	9444	mm ²
x	Cylinder Stroke	845	mm
f_f	Viscous Friction	90000	N.s/m
M	Mass	478.4	Kg

5 | DISCUSSION

The stepped rotary valve model used a nonlinear approach to show all the details of the valve construction and internal interactions³⁶ of the mechanical, fluid, electrical and electromagnetic parts. The disturbances were added to the valve model in the steady state flow mathematical expression given by Equation 27. A range of applied disturbances range from 0 to 1000 N/m is considered. Using 200 N/m disturbances force indicates that the MIM configuration is able to reject the fluid disturbances which is the obstacle in the traditional IM (Figure 9), that is, the MIM technique produces a better and more controllable performance compared with the full step technique. The performance error for the two models under the selected range of the inserted disturbances is shown in Figure 10.

Tests were performed on the five operation modes, with the parameters of the hydraulic actuator similar with the ones given by Shenouda¹⁹. It showed the selected operation mode by the algorithm, cylinder position, cylinder velocity, chambers flows, and chambers pressures. The mode switching and step division have been analysed for the system setup shown in Figure 11. It showed the ability to change between modes to save more energy. Regarding smoothness using step division, it indicated that there is a light change in the cylinder velocity performance.

6 | CONCLUSION

The IM is a hydraulic driving technique that is used to control the velocity of a hydraulic actuator such as a cylinder or a motor. Its main concept is represented by the control the meter-in and meter-out of the actuator configuration which allows energy recuperation or regeneration by recirculating fluid from one chamber to the another. Traditionally two main types of hydraulic control valve have been used to develop the IM system which are the linear spool valve and the poppet valve. A new stepped rotary valve has been developed to be embedded in the IM system. This valve has more stability and controllability because its design does not rely on the fluid to be a part of the valve control compared to the Valvistor type which depends on the fluid to control the valve. A comparison between the stepped valve and the traditional the poppet valve has been performed for simulated fluid disturbances. The results indicate that the new system is able to rejected these disturbances resulting in a improved stability of the valve.

References

1. Parr Andrew. *Hydraulics and pneumatics: a technician's and engineer's guide*. Elsevier; 2011.
2. Mattila Jouni, Koivumäki Janne, Caldwell Darwin G, Semini Claudio. A survey on control of hydraulic robotic manipulators with projection to future trends. *IEEE/ASME Transactions on Mechatronics*. 2017;22(2):669–680.
3. Edge KA. The control of fluid power systems-responding to the challenges. *Proceedings of the Institution of Mechanical Engineers, Part I: Journal of Systems and Control Engineering*. 1997;211(2):91–110.
4. Weber Jürgen, Beck Benjamin, Fischer Eric, et al. Novel system architectures by individual drives. In: ; 2016.

5. Schneider Markus, Koch Oliver, Weber Jürgen. Green Wheel Loader–improving fuel economy through energy efficient drive and control concepts. In: :8–10; 2016.
6. Hippalgaonkar Rohit, Ivantysynova Monik. A Series-Parallel hydraulic hybrid mini-excavator with displacement controlled actuators. In: no. 092:31–42Linköping University Electronic Press; 2013.
7. Lübbert Dipl-Ing Jan, Sitte Dipl-Ing André, Weber Ing Jürgen. Pressure compensator control–a novel independent metering architecture. In: :231–245; 2016.
8. Eriksson Björn, Palmberg Jan-Ove. Individual metering fluid power systems: challenges and opportunities. *Proceedings of the institution of mechanical engineers, part I: journal of systems and control engineering*. 2011;225(2):196–211.
9. Liu Song, Yao Bin. *Energy-saving control of single-rod hydraulic cylinders with programmable valves and improved working mode selection*. : SAE Technical Paper; 2002.
10. Kong Xiangdong, Shan Dongsheng, Yao Jing, Gao Yingjie. Study on experiment and modeling for the multifunctional integrated valve control system. In: :455–459IEEE; 2004.
11. Eriksson Björn. Control strategy for energy efficient fluid power actuators: Utilizing individual metering. PhD thesis-Linköping University Electronic Press2007.
12. Jansson Arne, Palmberg Jan-Ove. Separate controls of meter-in and meter-out orifices in mobile hydraulic systems. *SAE transactions*. 1990;:377–383.
13. Nielsen Brian Kongsgaard. Controller development for a separate meter-in separate meter-out fluid power valve for mobile applications. PhD thesisCiteseer2005.
14. Mattila Jouni, Virvalo Tapio. Energy-efficient motion control of a hydraulic manipulator. In: :3000–3006IEEE; 2000.
15. Hu Haibo, Zhang Qin. MULTI-FUNCTION REALIZATION USING AN INTEGRATED PROGRAMMABLE E/H CONTROL VALVE. *Applied engineering in agriculture*. 2003;19(3):283.
16. Yao Bin, DeBoer Chris. Energy-saving adaptive robust motion control of single-rod hydraulic cylinders with programmable valves. In: :4819–4824IEEE; 2002.
17. Lu Lu, Yao Bin. Energy-saving adaptive robust control of a hydraulic manipulator using five cartridge valves with an accumulator. *IEEE Transactions on Industrial Electronics*. 2014;61(12):7046–7054.
18. Tabor Keith A. *Optimal velocity control and cavitation prevention of a hydraulic actuator using four valve independent metering*. : SAE Technical Paper; 2005.
19. Shenouda Amir. Quasi-static hydraulic control systems and energy savings potential using independent metering four-valve assembly configuration. PhD thesisGeorgia Institute of Technology2006.
20. Laamanen M Sc Arto, Vilenius Matti. Is it time for digital hydraulics. In: ; 2003.
21. Ketonen Miikka, Linjama Matti. High flowrate digital hydraulic valve system. In: ; 2017.
22. Vukovic Milos, Murrenhoff Hubertus. The next generation of fluid power systems. *Procedia engineering*. 2015;106:2–7.
23. Eriksson Björn. Mobile fluid power systems design: with a focus on energy efficiency. PhD thesisLinköping University Electronic Press2010.
24. Crosser Jeffrey A. *Hydraulic circuit and control system therefor*. US Patent 5,138,838; 1992.
25. Smith David P, Mather Daniel T. *Electro-hydraulic metering valve with integral flow control*. US Patent 7,240,604; 2007.
26. Smith David P. *Electrohydraulic valve arrangement*. US Patent 5,868,059; 1999.
27. Hajek Jr Thomas J, Tolappa Srikrishnan T. *Independent and regenerative mode fluid control system*. US Patent 6,715,403; 2004.

28. Liu Song, Yao Bin. Programmable valves: a solution to bypass deadband problem of electro-hydraulic systems. In: :4438–4443IEEE; 2004.
29. Liu Song, Krutz Gary, Yao Bin. Easy5 model of two position solenoid operated cartridge valve. In: :63–67American Society of Mechanical Engineers; 2002.
30. Zhang Rong, Alleyne Andrew G, Prasetyawan Eko A. Performance limitations of a class of two-stage electro-hydraulic flow valves. *International Journal of Fluid Power*. 2002;3(1):47–53.
31. Yoo Benjamin, Hughes Eric Charles, Vance Rick Dean. *Method for calibrating independent metering valves*. US Patent 7,562,554; 2009.
32. Opdenbosch Patrick, Sadegh Nader, Book Wayne, Enes Aaron. Auto-calibration based control for independent metering of hydraulic actuators. In: :153–158IEEE; 2011.
33. EATON . *Ultrincs ZTS16 Twin Spool Valve*. Technical Catalog 1: EATON Powering Business Worldwide; 2010.
34. Rannow Michael. Fail operational controls for an independent metering valve. In: ; 2016.
35. Okhotnikov Ivan, Noroozi Siamak, Sewell Philip, Godfrey Philip. Evaluation of steady flow torques and pressure losses in a rotary flow control valve by means of computational fluid dynamics. *International Journal of Heat and Fluid Flow*. 2017;64:89–102.
36. Abuowda Karem, Noroozi Siamak, Dupac Mihai, Godfry Phil. A dynamic model and performance analysis of a stepped rotary flow control valve. *Proceedings of the Institution of Mechanical Engineers, Part I: Journal of Systems and Control Engineering*. 2019;:0959651818820978.
37. Abuowda Karem, Noroozi Siamak, Dupac Mihai, Godfrey Phil. Algorithm Design for the Novel Mechatronics Electro-Hydraulic Driving System: Micro-Independent Metering. In: :7–12IEEE; 2019.
38. Xu Bing, Ding Ruqi, Zhang Junhui, Cheng Min, Sun Tong. Pump/valves coordinate control of the independent metering system for mobile machinery. *Automation in Construction*. 2015;57:98–111.
39. Liu Kailei, Gao Yingjie, Tu Zhaohui. Energy saving potential of load sensing system with hydro-mechanical pressure compensation and independent metering. *International Journal of Fluid Power*. 2016;17(3):173–186.
40. Merritt Herbert E. *Hydraulic Control Systems*, John Wiley & Sons. New York, New York. 1967;.
41. Tabor Keith A. *A novel method of controlling a hydraulic actuator with four valve independent metering using load feedback*. : SAE Technical Paper; 2005.
42. Abuowda Karem, Noroozi Siamak, Dupac Mihai, Godfry Phi. Algorithm Design for the Novel Mechatronics Electro-hydraulic Driving System: Micro-Independent Metering. In: :7-12IEEE,IES,Thüringer Innovationszentrum Mobilität; 2019.
43. Bendjedia M, Ait-Amirat Y, Walther B, Berthon A. Sensorless control of hybrid stepper motor. In: :1–10IEEE; 2007.
44. Kepiński Radosław, Awrejcewicz Jan, Lewandowski Donat. Dynamical simulation of a nonlinear stepper motor system. *International Journal of Dynamics and Control*. 2015;3(1):31–35.
45. Luo Yamin. System modeling and control design of a two-stage metering poppet-valve system. PhD thesisUniversity of Missouri–Columbia2006.
46. Muller Matthew. Modeling, design and control of forced-feedback metering poppet valve system. PhD thesisUniversity of Missouri–Columbia2006.
47. Hansen Anders Hedegaard, Schmidt Lasse, Pedersen Henrik C, Andersen Torben O. A generic model based tracking controller for hydraulic valve-cylinder drives. In: :V001T01A016–V001T01A016American Society of Mechanical Engineers; 2016.

How to cite this article: Karem Abuowda., M. Dupac, S. Noroozi, and P. Godfrey , Mathematical Methods in the Applied Sciences, (2020)

This work does not have any conflicts of interest

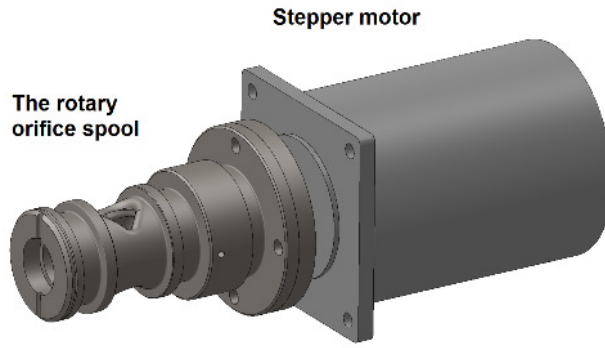


FIGURE 1 Stepped rotary flow control valve

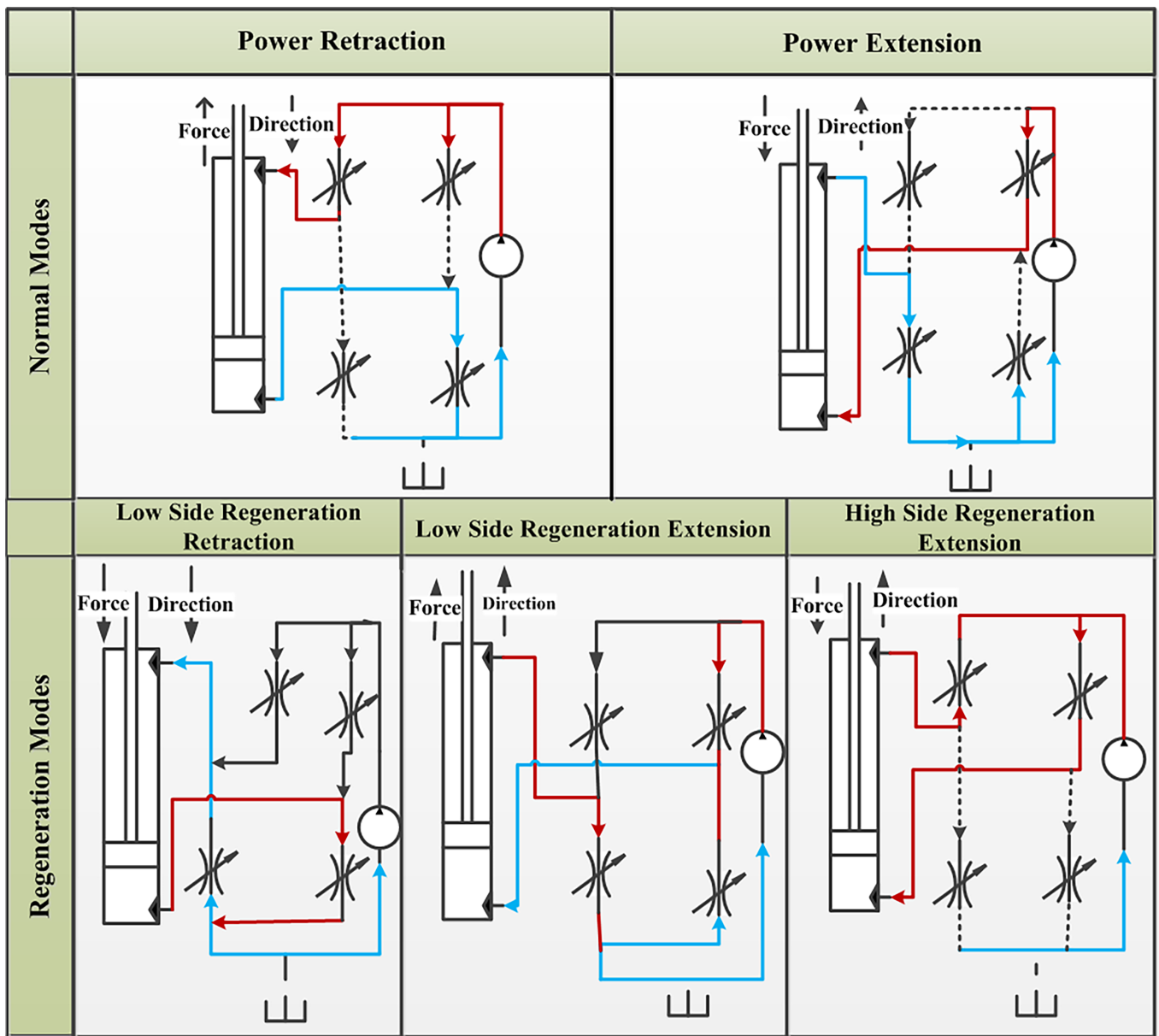


FIGURE 2 The physical representation of the Independent Metering operation modes

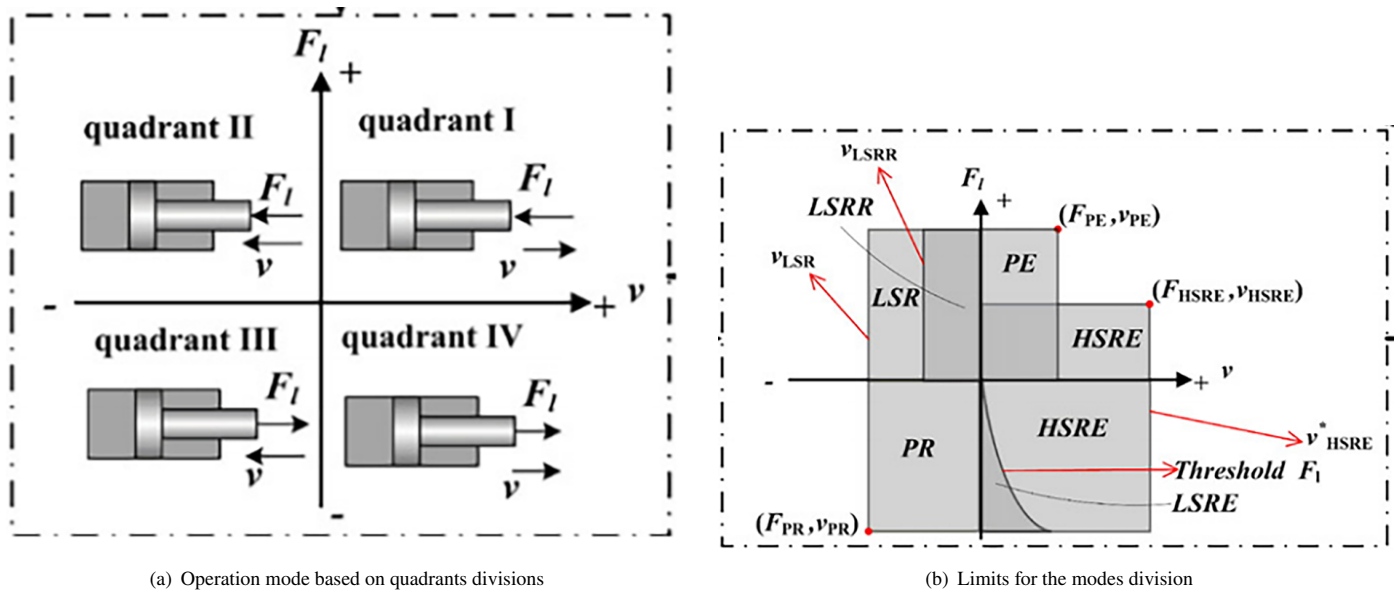


FIGURE 3 Limitation for the operation modes in IM

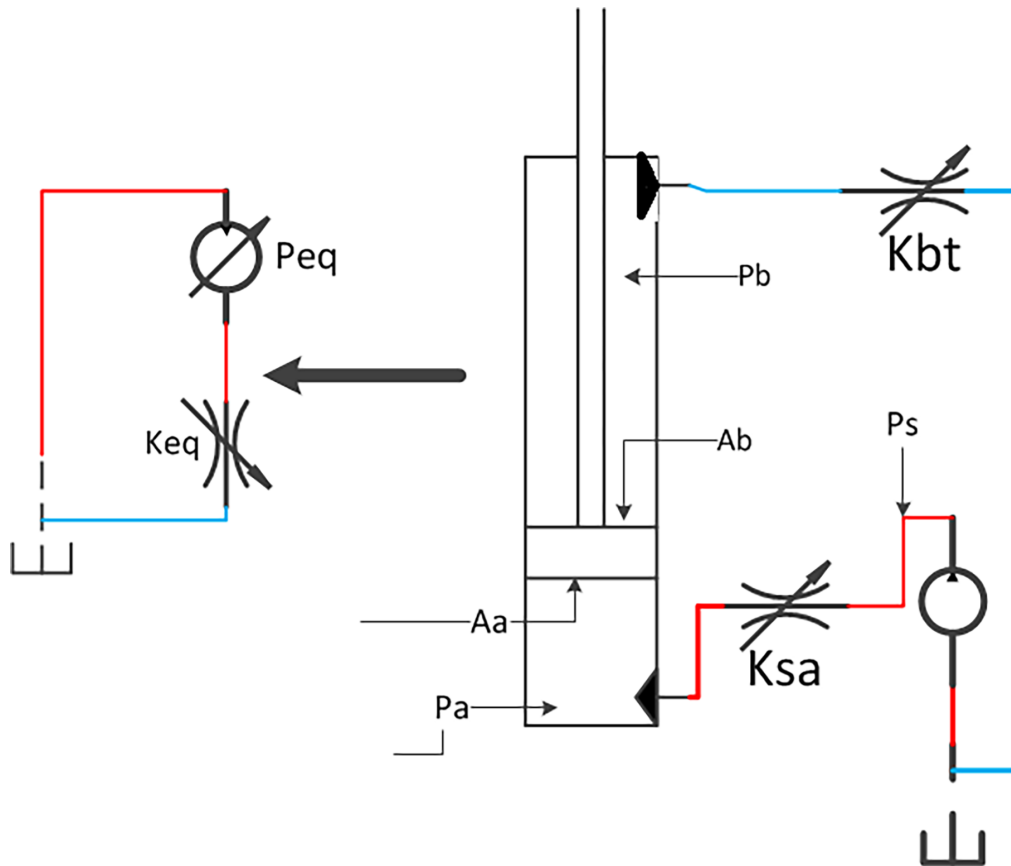


FIGURE 4 The equivalent circuit for the power extension mode³⁹

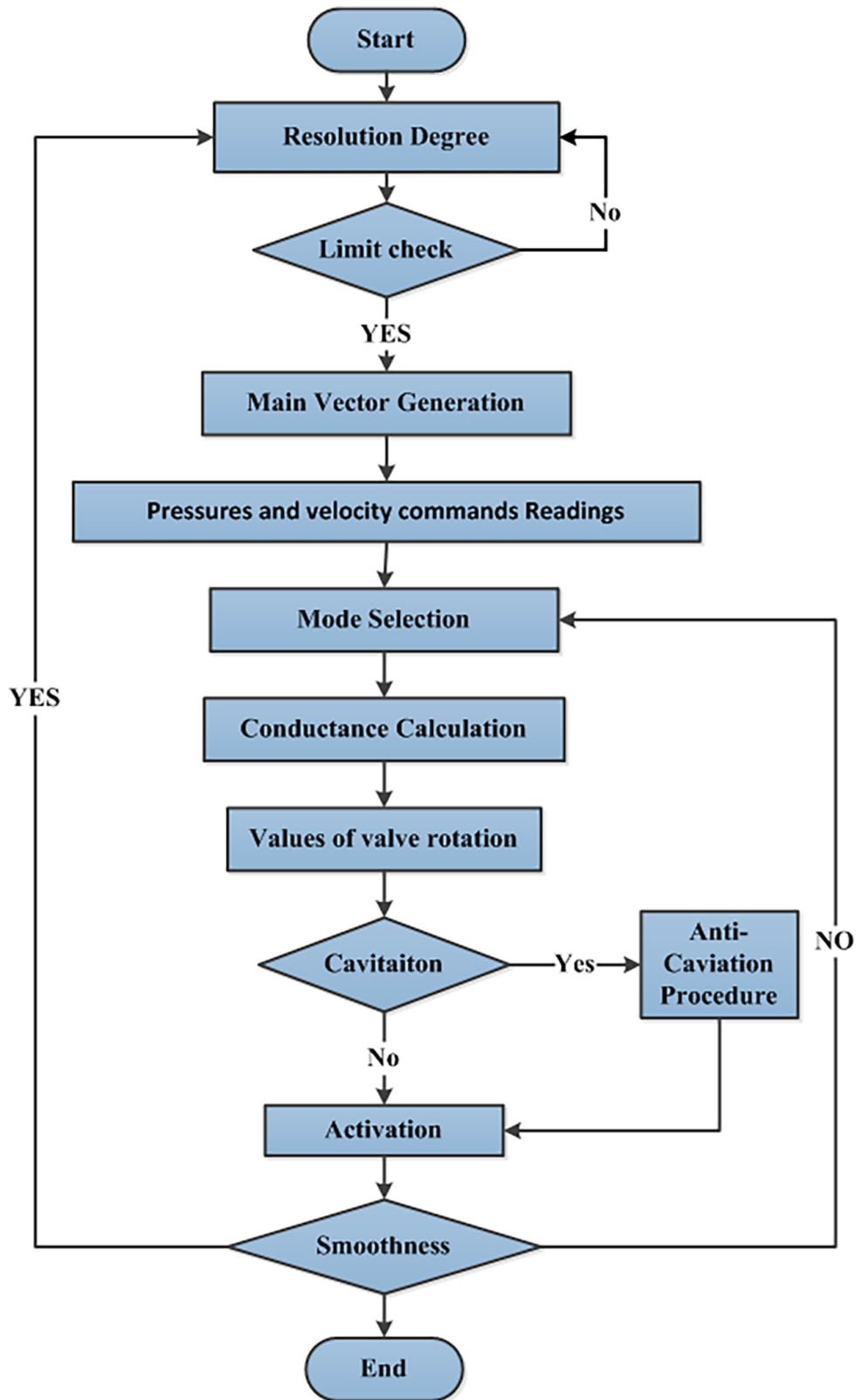


FIGURE 5 The MIM control algorithm flowchart

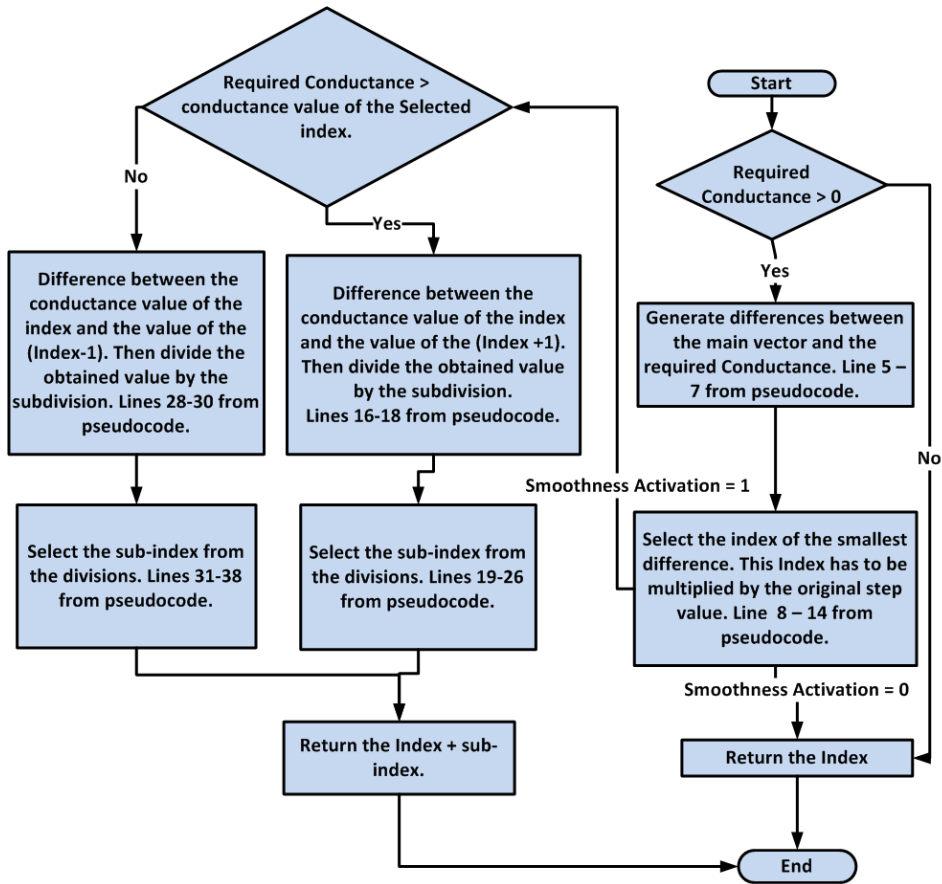


FIGURE 6 The Close Value Detection Algorithm developed for the MIM system

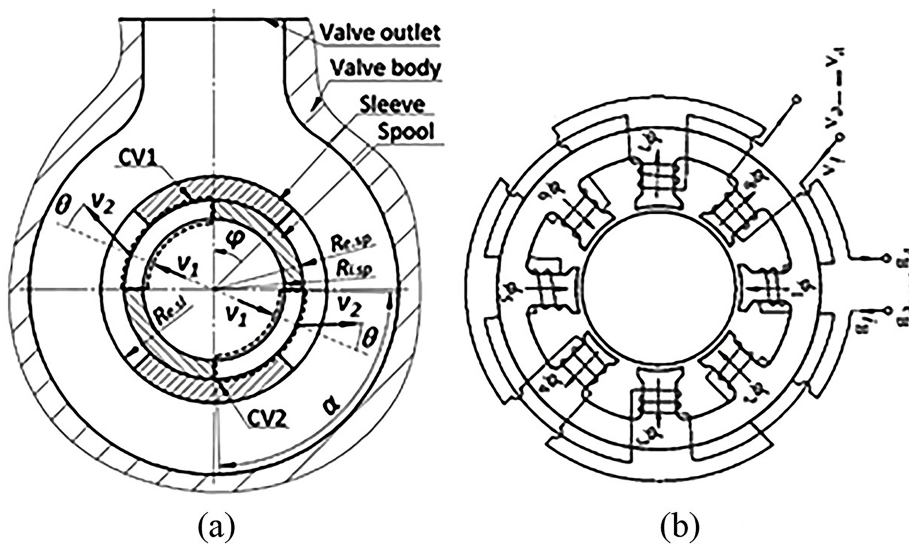


FIGURE 7 Schematic diagram of the valve two main parts which are the mechanical orifice and the stepper motor respectively³⁶

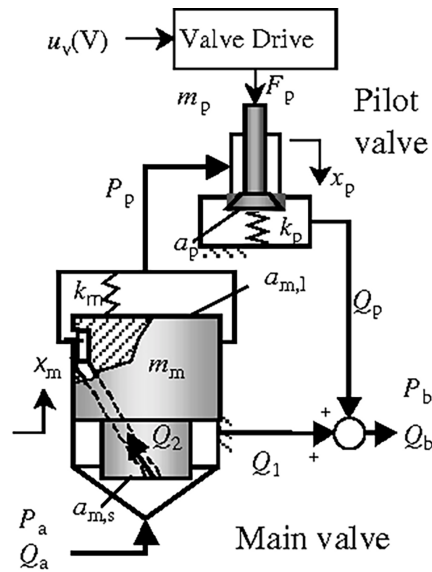


FIGURE 8 The schematic diagram of the Valvistor valve

Velocity Performance comparison between the novel MIM system and the traditional system

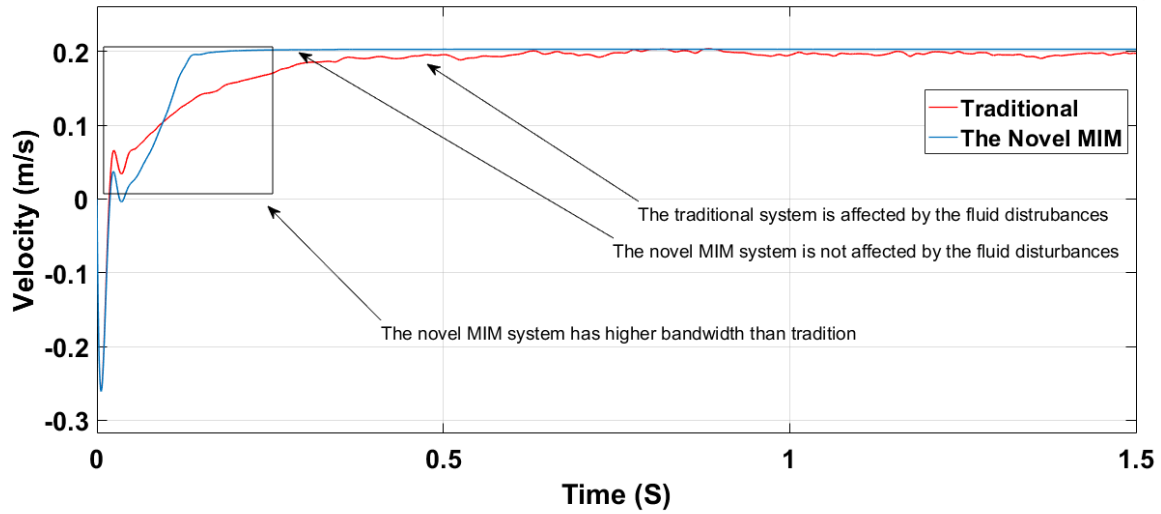


FIGURE 9 The velocity performance between the MIM configuration and traditional IM under fluid disturbances effect.

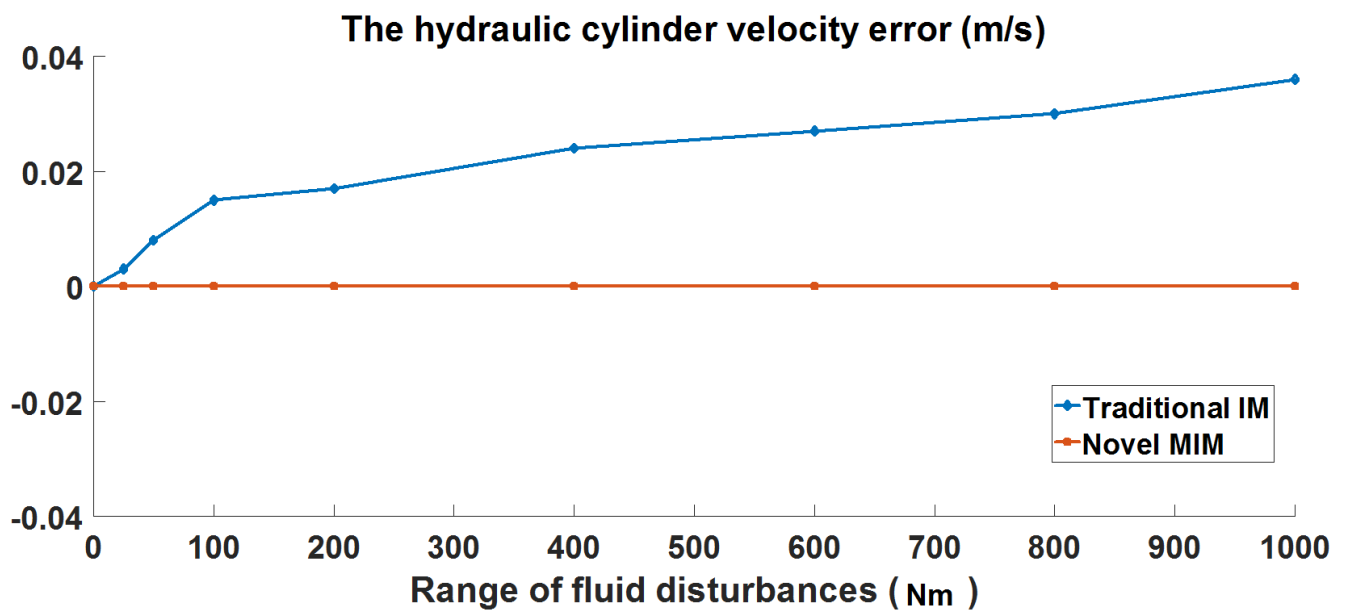


FIGURE 10 The velocity performance error for the two systems IM and MIM models under effect of a range of generated disturbances

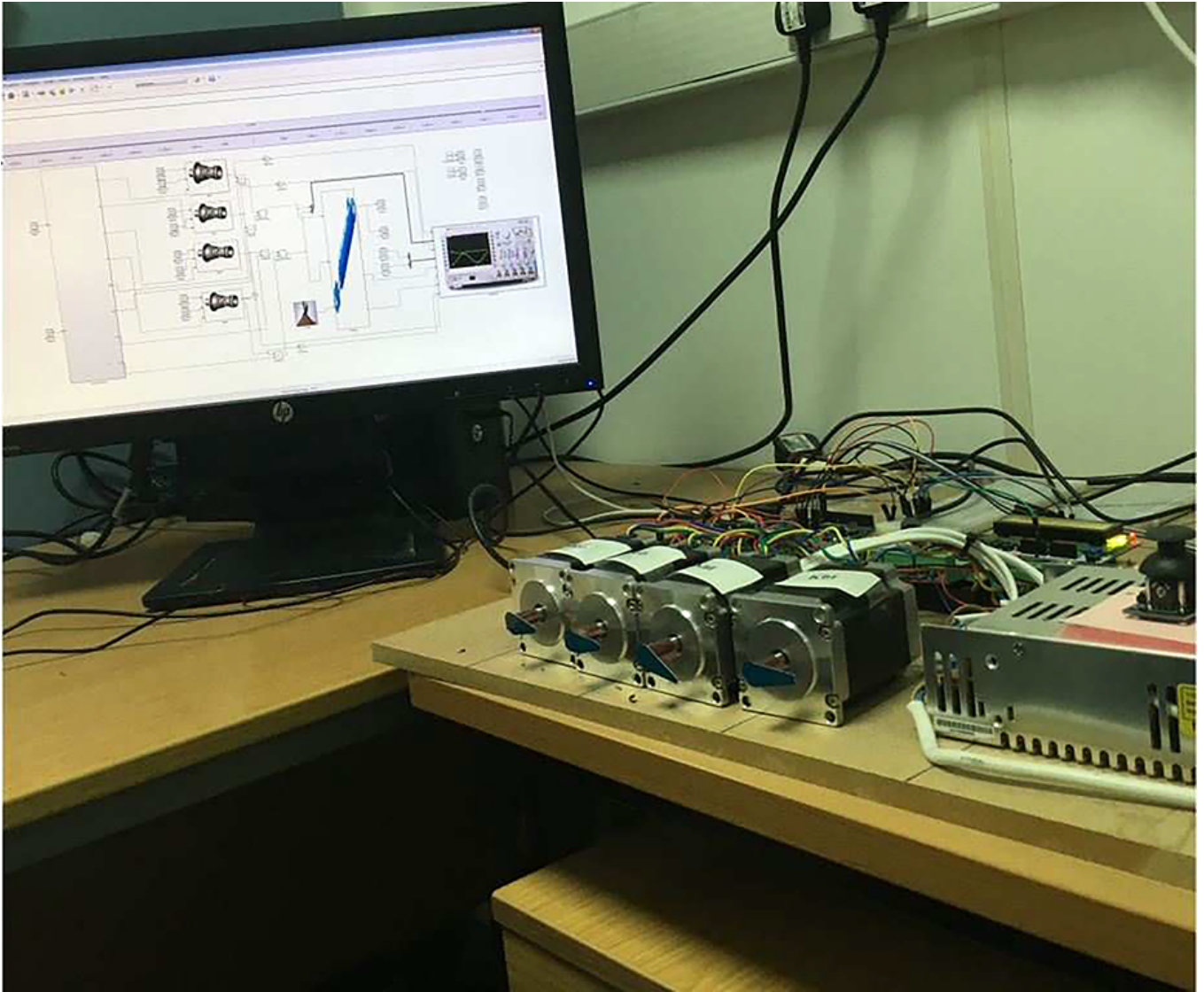


FIGURE 11 System setup for operation mode, mode switching and step division